Investigation of the Hemodynamics Influencing Emboli Trajectories Through a Patient-Specific Aortic Arch Model

Article *in* Stroke · April 2019

DOI: 10.1161/STROKEAHA.118.023581

6 authors, including:

Fiona Malone
Galway-Mayo Institute of Technology
10 PUBLICATIONS **12** CITATIONS
SEE PROFILE

Eugene Mccarthy
Galway-Mayo Institute of Technology
25 PUBLICATIONS **134** CITATIONS
SEE PROFILE

Patrick Delassus
Galway-Mayo Institute of Technology
41 PUBLICATIONS **441** CITATIONS
SEE PROFILE

J-H Buhk
University Medical Center Hamburg - Eppendorf
132 PUBLICATIONS **966** CITATIONS
SEE PROFILE

Original Contribution

Investigation of the Hemodynamics Influencing Emboli Trajectories Through a Patient-Specific Aortic Arch Model

Fiona Malone, PhD; Eugene McCarthy, PhD; Patrick Delassus, PhD; Jan-Hendrick Buhk, MD; Jens Fiehler, MD; Liam Morris, PhD

Background and Purpose—Cardiogenic emboli account for 15% to 20% of acute ischemic stroke cases worldwide. However, the chance of such emboli, of varying sizes, causing a stroke under various flow types has not been evaluated.

Methods—A patient-specific aortic arch model was fabricated from a medical image dataset of a 77-year-old male case, with atrial fibrillation and distal occlusion of the right M1 vessel. One hundred and eighty mammalian embolus analogs (EAs) were released one by one into the model under normal and atrial fibrillation flow conditions. A further 270 clots were fabricated using varying levels of thrombin (5–20 National Institute of Health units thrombin). The effect of releasing several clots simultaneously was also examined by grouping EAs into 18 multiples of 5, 4, 3, and 2 clots, resulting in 504 EAs released.

Results—EAs with a length of ≤10 mm were the most common geometry to travel through the common carotid arteries (44%); however, longer clots also traveled through these narrow vessels. Twenty two percent of EAs ranged from 10–20mm in length, 27% from 20–30mm and 7% were >30 mm in length. Higher density clots increased the propensity for clots to travel along the cerebral vessels ($P<0.05$). Releasing more clots during each test, increased the probability of at least one clot traveling through an aortic arch branching vessel.

Conclusions—Embolus trajectory through the branching vessels of the aortic arch is not exclusively dependent on embolus size. EAs tend to travel proportionally with outlet flow rates, with a greater chance of a stroke caused by multiple breakaway emboli.

Visual Overview—An online visual overview is available for this article. **(*Stroke*. 2019;50:00-00. DOI: 10.1161/STROKEAHA.118.023581.)**

Key Words: aorta ■ atrial fibrillation ■ embolism ■ hemodynamics ■ stroke

The origin, composition, and size of stroke-causing embolic clot(s) within the cerebral vasculature are still unclear. Clots may originate from various sources, ranging from one to multiple clot blockage(s). Worldwide, cardiogenic embolisms account for ≈15% to 20% of acute ischemic strokes.[1,2] Atrial fibrillation (AF) is the most significant contributor to cardiogenic emboli formation, causing 45% of all cardioembolic strokes.[3,4] Choi et al[5] showed that AF can increase the incidence of carotid embolism. They applied computational fluid dynamic techniques which simulated rigid spheres within an idealized, rigid wall aortic arch model comprising of the 3 branching vessels. Their simulations demonstrate that stroke propensity was significantly affected by sphere diameter, as well as hemodynamic waveforms.

Cardiogenic emboli can range in size from a few millimeters to 4 cm.[6] Smaller sized clots travel proportionally to the flow,[7] whereas larger sized clots are prone to travel along the much larger middle cerebral artery rather than the smaller anterior cerebral artery.[7–10]

This study provides clarity on cardiogenic emboli trajectory paths by using an AF patient-specific, aortic arch model. The trajectory patterns of small and large mammalian embolus analogs (EAs) of various thrombin concentrations were assessed under normal and AF flow conditions. Inducing EAs with thrombin allows for control over the fibrin content. It must be noted that the exact coagulation system of the human is not modeled and, therefore, is excluded from its effects on thrombus fate (where and whether dissolution takes place). This study specifically removes all protein and protease constituents of the plasma and the circulating cells. The antithrombotic characteristics of the vasculature are also uninvolved and likewise cannot be accounted for by this experimental setup.

These trajectory tests will provide a greater understanding into whether or not cardiogenic emboli travel proportionally

Received June 20, 2018; final revision received February 7, 2019; accepted March 13, 2019.

From the GMedTech, Department of Mechanical and Industrial Engineering, Galway-Mayo Institute of Technology, Galway, Ireland (F.M., E.M., P.D., L.M.); and

Department of Diagnostic and Interventional Neuroradiology, University Medical Center Hamburg-Eppendorf, Martinistr, Germany (J.-H.B., J.F.).

The online-only Data Supplement is available with this article at https://www.ahajournals.org/doi/suppl/10.1161/STROKEAHA.118.023581.

Correspondence to Fiona Malone, PhD, GMedTech, Department of Mechanical and Industrial Engineering, Galway-Mayo Institute of Technology, Galway, Ireland. Email fiona.malone@gmit.ie

with flow regardless of clot size, morphology, quantity, or change in pulsatile flow conditions. A greater knowledge of these relationships will assist computer simulations in predicting the likelihood of a patient's propensity of stroke and ultimately the lodgment location of a cardiogenic embolism.

Methods

The authors declare that all supporting data are available within the article. The ethics committee waived the need for patient consent and approved the study.

Aortic Arch Model

A medical image dataset of an aortic arch for a 77-year-old male case, with AF and distal occlusion of the right M1 vessel, was obtained from the University Medical Centre Hamburg-Eppendorf, Germany. The commercially available, image reconstruction software, Mimics (Materialise, Leuven, Belgium) was used to generate a 3-dimensional mask, saved in stereolithography format (Figure 1A) by applying various segmentation and smoothing methods.[8] This arch was of a Romanesque shape which is presented in over 80% of patients[11] with Type II branching.[12] Cylindrical sections were added to the ascending and descending aorta to create easier connection points with commercially available tubing for in vitro testing. The image dataset did not include sufficient ascending aortic arch length because the scanning protocol did not include the aortic valve and portion of the proximal ascending aorta. Therefore, a cylindrical section was added to replace the missing ascending aorta section, thus eliminating the true vessel curvature of that section.

The model core was 3-dimensional printed in Watershed stereolithographic material (LPE 3D printing, Belfast, Ireland; Figure 1B), which created a 2-part silicone mold to cast low melting point alloy cores. These were painted in layers with Elastosil 4641 silicone with Thivex silicone thickener (Wacker Chemie AG) to achieve wall thickness of 2 mm, and 1.5 mm for the branching vessels.[13] The Young modulus of the silicone mixture was 1.04±0.098 MPa, which was within the range for typical aortic tissue.[14,15] The low melting point alloy was melted to reveal a thin-walled, flexible and compliant patient-specific aortic arch model (Figure 1D).

The silicone model had a compliance value of 0.0006 mm Hg^{-1} which was within physiological range for aortic arch tissue.[16] There was no significant difference in compliance between normal and AF flow conditions (Methods in the online-only Data Supplement for details on compliance definition).

Physiological Flow Replication

The replication of normal ascending aorta flowrate was based on previously published data.[17] The flow rate graph was scanned and digitized using Matlab v 7.0.1 (Mathworks) (Figure 2A). Clark et al[18] clinically observed an average reduction in normal cardiac output and pulse period by 30 and 40%, respectively, for AF conditions. The normal cardiac output and cycle length[17] were scaled down to achieve a feasible AF velocity profile (Figure 2A). This method was also applied by Choi et al[5] for numerical studies.[5]

A blood mimicking fluid mixture of glycerin and water in a ratio of 40:60 by weight displayed similar properties to human blood with a density of 1058.33 kg·m^{-3} at 21.1°C and a viscosity of 3.7 mPas, as measured by a cone and plate viscometer (Brookfield DV-II+Pro). The fluid was pumped through the aortic arch model in a closed loop system. Two ultrasonic flow meters (25 PXL flow sensor; 16PXL Clamp-on flow sensor, Transonic) monitored inlet and outlet flowrates (Figure 2B and 2C). The average flow rates were within normal physiological ranges for the right/left subclavian artery (400–500 mL),[19,20] common carotid arteries (CCAs; 363±18 mL·min^{-1}), and vertebral arteries (90±12 mL·min^{-1}).[21] The percentage outlet flowrate through the descending aorta varied from 70% to 73% which is within the clinical range.[22,23] The pressure was maintained within physiological levels as monitored by a pressure transducer (Model FDW; R.D.P Electronics Ltd, Sole, United Kingdom; Figure 2B and 2C).

Cardiogenic Embolus Analogues

Bovine blood was obtained from a local abattoir (Burkes, Gort, Galway, Ireland), a European Union approved abattoir supervized by Galway County Council, Ireland, veterinary services. Bovine thrombin (Sigma Aldrich) was used as the clotting mechanism, ranging from 5 to 20 National Institute of Health units (NIHU).

Density (ρ) is given by the ratio of mass (m) to volume (V):

$$\rho = \frac{m}{V} \quad (1)$$

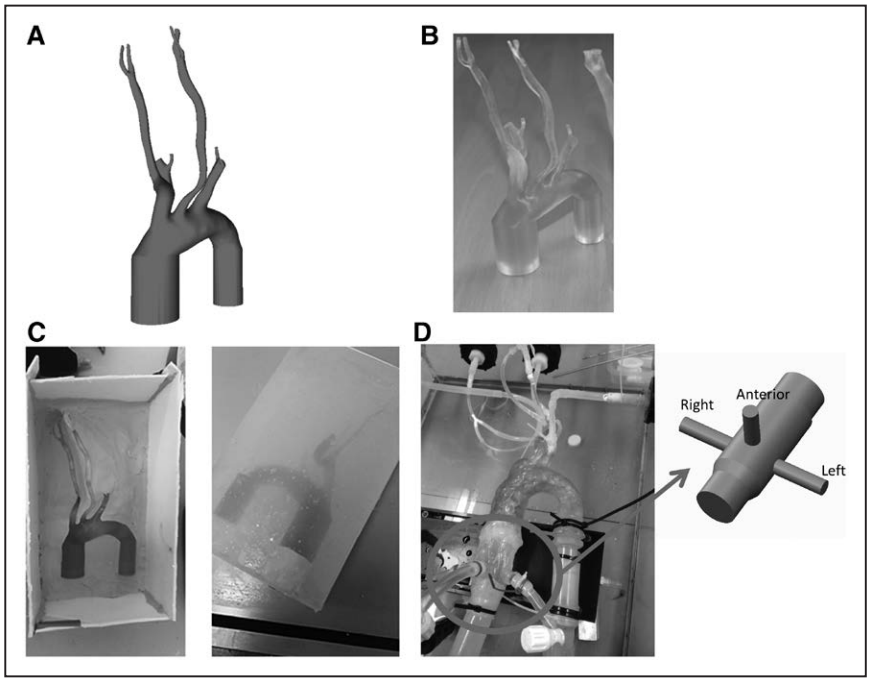

Figure 1. This Figure displays the process by which the model was fabricated. **A**, Three-dimensional (3D) mask of 2-dimensional patient dataset using Mimics (Materialise); (**B**) 3D printed patient-specific model; (**C**) 2-part mold creation with silicone block mold; (**D**) flexible 3D patient-specific model with 3-way connector and branching vessels located within the simulation system.

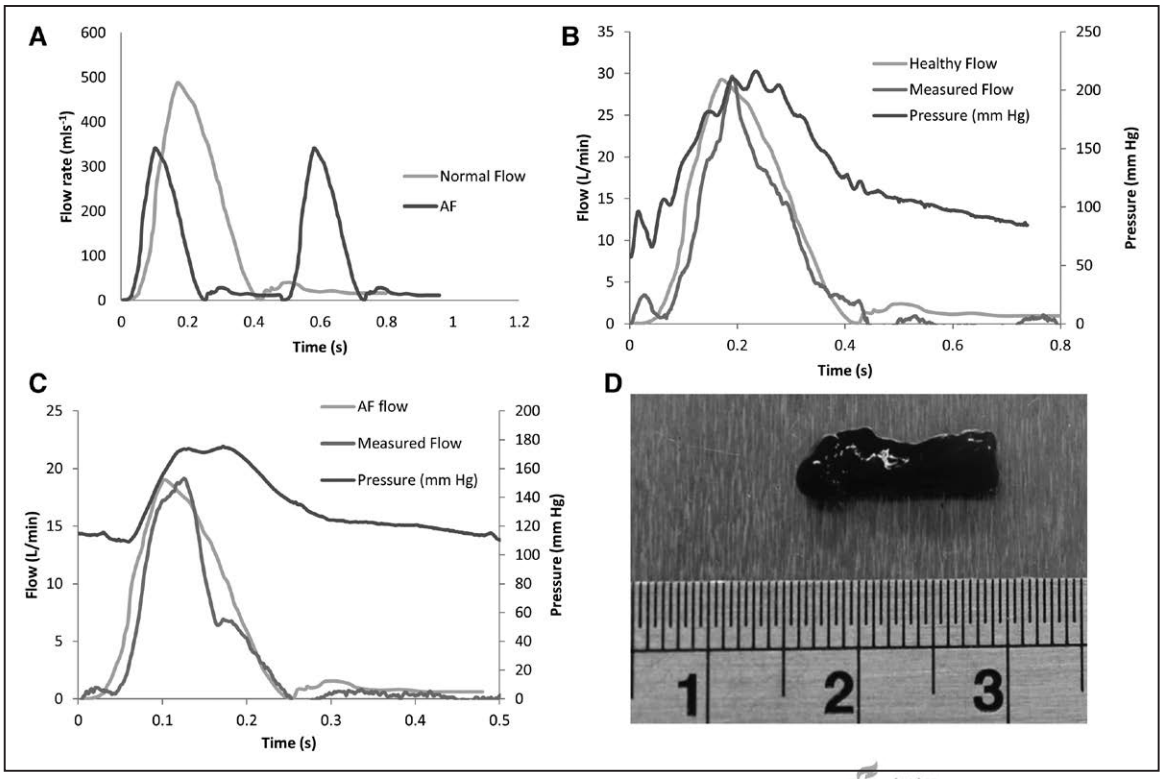

Figure 2. **A**, Velocity profiles for healthy (light gray) and atrial fibrillation (AF; dark gray) flow conditions as recorded in literature; (**B**) recorded healthy pulsatile flow and pressure (single pulsation); (**C**) recorded AF pulsatile flow and pressure (single pulsation); (**D**) embolus analog.

The volume was measured by clotting blood within a graduated vessel and then weighing the sample on an electronic balance, subtracting the vessel mass.

Young modulus (E) refers to the ratio between stress (σ) and strain (ε)

$$E=\frac{\sigma}{\varepsilon} \quad (2)$$

The higher the Young modulus, the stiffer the material. The EAs (Figure 2D) displayed a compressive Young modulus varying from 1.53 to 16.6 kPa for a percentage strain range of 5% to 40%,[24] similar to other compressive studies for human retrieved emboli.[25] EA stiffness also increased with addition of thrombin.[26] (Methods in the online-only Data Supplement for details on histological testing).

Two cameras (50 Hz frame rate, 12 MPixels) were used to monitor EA trajectories. A flexible connector allowed the clots to be released from the left, right, and anterior positions (Figure 1D). EAs were released at the beginning of each cardiac cycle through a primed, 3-way connector. One hundred and eighty EAs, with lengths of 11.84±8.24 mm and diameters of 4.66±1.11 mm, as measured by an electronic digital calipers (Maplin, England) with an accuracy of 0.01 mm, were released one by one into the physiological simulation system under normal (90 EAs) and AF (90 EAs) flow conditions. Thirty EAs were released through the left, right, and anterior entry positions for both flow conditions. A further 270 clots were fabricated using varying levels of thrombin (45 EAs with 5, 10, and 20 NIHU), with 15 EAs released at the left, right, and anterior positions.

The effect of releasing a number of clots simultaneously was examined. EAs were grouped into 18 multiples of 5, 4, 3, and 2 clots. Each group was released through the left, right, and anterior positions 6× resulting in 252 released EAs. Table I in the online-only Data Supplement displays the number and use of clots for the various experimental set-ups.

The χ^2 test assessed the hypotheses whether EA trajectories are distributed proportionally to flowrate type, EA composition, and quantity of EAs traveling along each branching vessel. In all cases, the experimental data was compared with the null hypothesis (uniform distribution of EAs) using a χ^2 goodness-of-fit test within Minitab 17.0 (Minitab, Inc, State College, PA).

Results

Healthy Pulsatile Flow Versus AF Pulsatile Flow (No Thrombin)

Table II in the online-only Data Supplement displays the number of EAs traveling along the outlet vessels for 1 EA released from the right, anterior, and left entry locations for both flow conditions and various thrombin concentrations. Figure 3 displays a schematic of the trajectory paths. For the EAs that were not fabricated with thrombin (0 NIHU), there was a decreased number of EAs traveling through the descending aorta under AF flow conditions and a subsequent increase in EAs traveling through the branching vessels. There was a significant difference in clot trajectory paths under AF flow conditions when compared with healthy flow, χ^2 (1, N=180)=4.13; $P<0.05$. Twenty-seven EAs out of 180 clots traveled through the CCAs, with more than double the number traveling through the left common carotid artery (LCCA; 20 EAs) than the right common carotid artery (RCCA; 7 EAs). Smaller EAs with a length ≤10 mm were the most common geometry to travel through the CCA vessels (12 EAs, 44%); however, longer clots passed through these narrow vessels. Six EAs (22%) were between 10 and 20 mm, 7 EAs (27%) between 20 and 30 mm, and 2 EAs (7%) longer than 30 mm. There was no significant difference in trajectory paths when EAs were released from the left, anterior, and right positions.

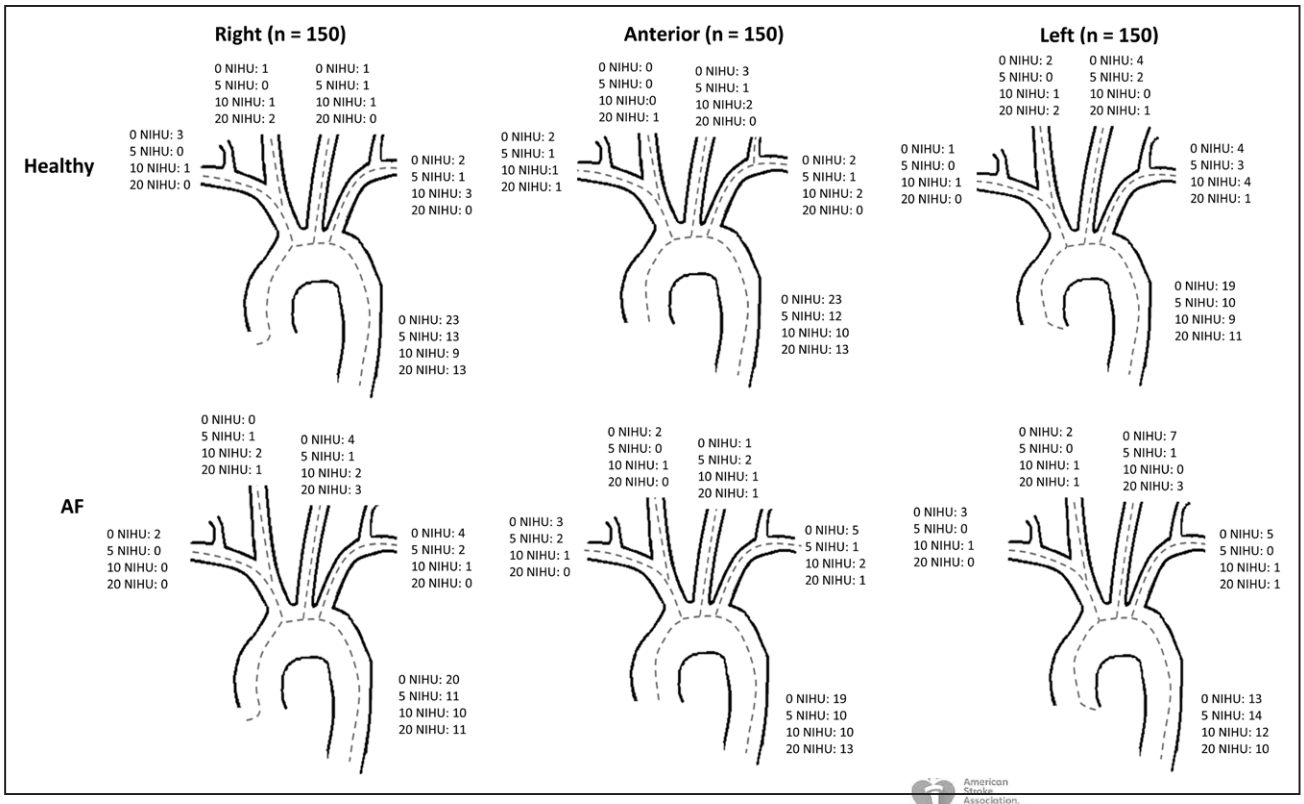

Figure 3. Schematic of single embolus analogue trajectory paths with varying thrombin concentrations (n=450), as released from right (0 NIHU; n=30; 5 NIHU (n=15); 10 National Institute of Health units (NIHU; n=15); 20 NIHU (n=15)), anterior (0 NIHU; n=30; 5 NIHU (n=15); 10 NIHU (n=15); 20 NIHU (n=15)) and left (0 NIHU; n=30; 5 NIHU (n=15); 10 NIHU (n=15); 20 NIHU (n=15)) through the model under healthy and atrial fibrillation (AF) conditions.

Effect of Thrombin Concentration on EA Trajectory Path

Figure 4A shows the histological analysis of the thrombin-induced bovine emboli at 0, 5, and 10 National Institutes of Health stained using hematoxylin and eosin and martius scarlet blue at ×40 magnification. Using ImageJ, the erythrocyte cell count ranged from 74.96% to 82.30% among the samples tested by hematoxylin and eosin staining. Under martius scarlet blue staining, the presence of fibrin increased from 3.55% (0 NIHU) to 47.48% (10 NIHU). The density of the clots also increased with increasing thrombin concentrations (Figure 4B). Figure 3 displays the trajectory paths for varying thrombin concentrations (0–20 NIHU). The variation in thrombin concentration was significant in affecting the clot trajectory paths through the branches and the descending aorta when compared with clots not induced with thrombin, χ^2 (3, N=450)=9.60, P<0.05. Figure 4C shows the overall increase in clots traveling through the LCCA and RCCAs towards the cerebral vasculature, for AF flow conditions and increased thrombin concentration.

Multiple EAs Released Per Test

Figures 5A and 5B display the percentage of clots that traveled through the branching vessels under healthy and AF flow conditions, respectively, when clots were released individually or in groups of multiple clots. Releasing multiple clots at a time increased the probability of at least 1 clot traveling through the branching vessels supplying the brain from 27% to 83% when 5 clots were released, from 12% to 72% when 4 and 3 clots were released and from 27% to 45% when 2 clots were released, under normal flow conditions. AF flow conditions increased the number of EAs that traveled through the branching vessels. On 2 occasions, all released clots traveled through the branching vessels (5 clots: AF; 2 clots: AF). Figure 6 displays an overall schematic of the trajectory paths for the released multiple EAs.

Discussion

To the best of our knowledge, there are currently no simulations presented in the literature that release and track cardioembolic trajectory paths under normal and AF flow conditions through compliant patient-specific aortic arch models, which incorporate the branching vessels. The aortic arch model was of a normal, rounded, Romanesque geometry. This shape is the most common aortic arch geometry throughout the global population (80%) and displayed the most common 3-branch pattern of the brachiocephalic trunk, LCCA, and left subclavian arteries.[26]

The 77-year-old patient with AF had a distal occlusion of the right M1 vessel. The risk of cardiogenic embolism varies even within the patient's individual cardiac abnormalities. For example, in patients with AF, associated heart disease, age, duration of arrhythmia, chronic versus intermittent fibrillation, and atrial size all influence this embolic risk.[27] It is possible that the presence of a possible cardiac source of embolism does not necessarily mean that the stroke was caused by an embolus from the heart. Simultaneous atherosclerosis of the CCAs is another common cause of stroke in such patients.[28] However, the dataset obtained is a good foundation for the investigation into cardioembolic stroke.

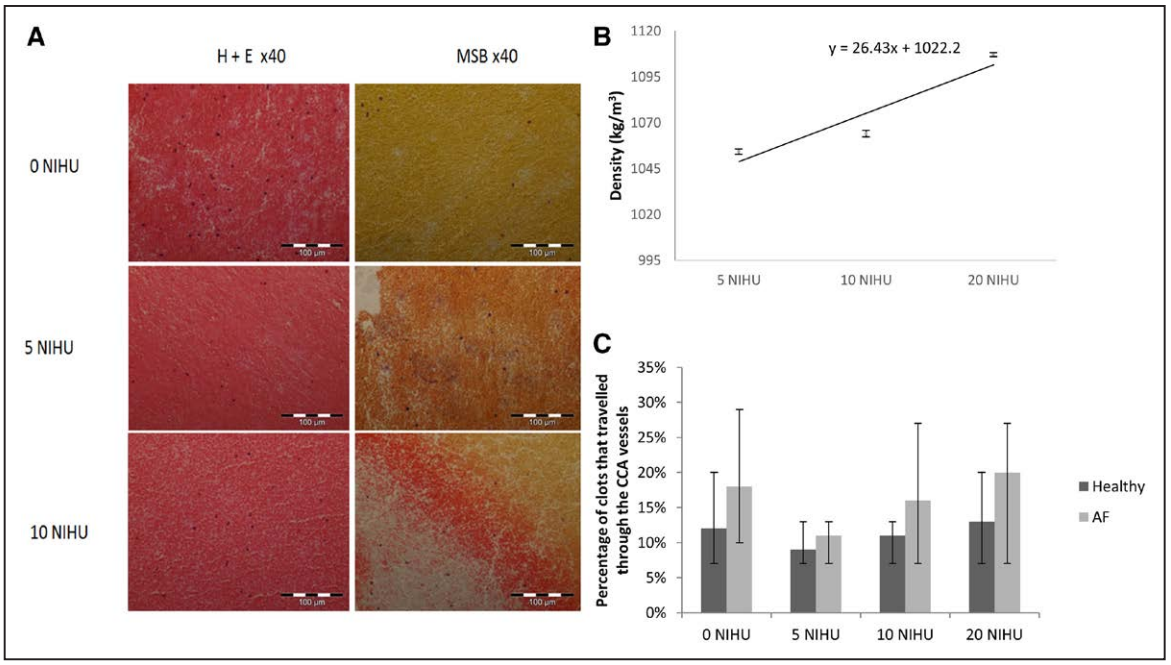

Figure 4. **A**, Thrombin-induced bovine thrombi at 0, 5 and 10 NIHU stained using hematoxylin and eosin and martius scarlet blue at ×40 magnification; (**B**) increase in density with increasing levels of thrombin. The error bars show the range based on 5 individual tests; (**C**) bar chart of the number of thrombin-induced clots that traveled through the common carotid artery (CCA) vessels. The error bars show the range based on 3 individual tests (1 for each position, **left**, **right**, and **center**). AF indicates atrial fibrillation.

Seven hundred and two bovine EAs were fabricated for this study to simulate cardiac source clot trajectory paths. The mechanism of coagulation is universal across mammalian biology.[29] Ovine, porcine, and bovine blood is the most frequently used mammalian blood for EA replication.[25,30–33] Bovine blood was chosen for EA manufacture as the supply was in close proximity to the laboratory (Burkes Abattoir, Ltd, Galway) and, on a macro level, the composition of bovine blood is similar to human blood.[34] Biochemically, there are variations in animal and human blood, but these do not alter the performance of bovine blood as a simulator for human blood, as activity of the tissue factor pathway, and fibrinolytic system in cattle is within human range.[35]

In cases of cardiogenic emboli as a result of AF, these emboli tend to originate in areas of stagnation and low flow regions, resulting in a high percentage of red blood cells present in the emboli. Inducing bovine EAs with thrombin in static conditions[24] attempts to mimic such emboli and allows for control over the variance in clot composition, particularly fibrin. The bovine EAs displayed similar compositional structures to human specimens retrieved from stroke treatment procedures under hematoxylin and eosin and martius scarlet blue histological staining.[25] The dark blue-purple leukocytes are distributed in a similar fashion to that of the human specimen throughout the section.[25] Under visual inspection, the EAs were histologically similar to human thrombi retrieved from patients with stroke[25,36] and manufactured mammalian EAs under static conditions.[25,37]

Liebeskind et al[36] also quantified the composition of thrombi retrieved from patients with acute ischemic stroke. The thrombi retrieved were predominantly composed of fibrin (61±21%) and erythrocytes (34±21%). With increasing

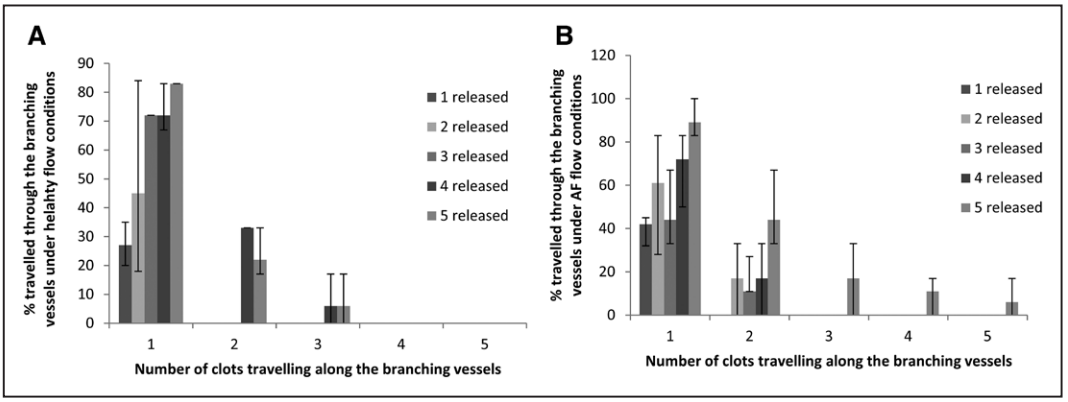

Figure 5. Percentage of clots traveling through the branching vessels per test under (**A**) healthy flow (n=252) and (**B**) atrial fibrillation (AF) flow conditions (n=252). The error bars were based on 3 individual tests (1 for each position: **left**, **right**, and **center**).

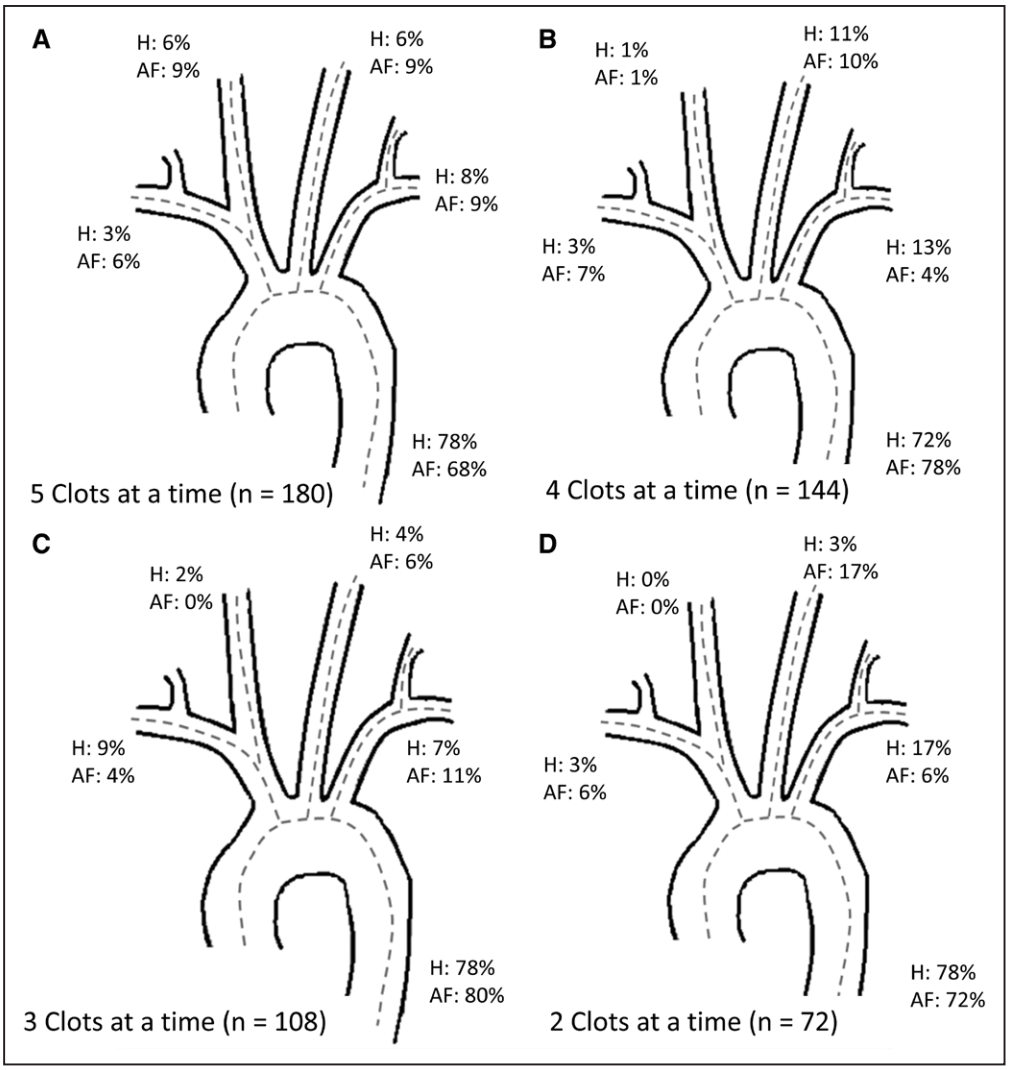

Figure 6. Schematic of multiple EA trajectory paths through the model under both flow conditions. AF indicates atrial fibrillation; and H, healthy flow conditions.

thrombin concentration, the composition of the cellular components of bovine EAs lie within their range. The addition of thrombin increased sample density and improved the specimen stability. It was observed that EAs induced with low concentrations of thrombin had lower structural integrity than those induced with higher thrombin concentrations and were predisposed to fragment or fracture. The bovine EAs were suitable models for replicating cardiogenic emboli and provided an improvement to previous models used to simulate emboli.[7,8]

Under healthy flow conditions, the majority of individually released EAs fabricated without thrombin traveled along the descending aorta (72%) with 12% of EAs traveling along the LCCA and RCCA which could ultimately lodge within the cerebral vasculature. There was a 2.7-fold increase in the number of EAs that traveled through the LCCA when compared with the RCCA. This patient had a stroke from a clot traveling along the RCCA, which was of a lower probability of occurring based on our setup. Twelve percent of the total flow traveled through the LCCA and RCCA, and 14% traveled through the left/right subclavian arteries. It is evident that the EA trajectory paths were proportional to the percentage flowrate through these branching vessels. There was a significant decrease in the number of EAs, fabricated without thrombin, that traveled through the descending aorta under AF flow conditions when compared with healthy flow conditions, χ^2 (1, N=180)=4.13; $P<0.05$. All branching vessels experienced an increase in the number of EAs under AF flow conditions.

The 27 clots that traveled through the CCA ranged in lengths from 4.24 mm to 37.83 mm, falling within the physiological range of atrial and appendage thrombi found in patients.[38] It was evident that larger emboli indeed have the ability to change geometry to fit through narrower blood vessels, and it is highly conceivable that these sized clots can occlude the distal vessels in the occurrence of acute ischemic strokes. Fragmentation of the EAs also occurred. It was observed that large and small-sized clots, with and without the addition of thrombin, had the ability to split resulting in part of the clot traveling along the branching vessels and descending aorta. This occurred 3% of the time on average.

The addition of bovine thrombin reduced fragmentation because of the increase in material density and was a significant contributor in the overall variation of all singular clot trajectories when compared with EAs fabricated without

thrombin, $\chi^2(3, N=450)=9.60$; $P<0.05$. This could be attributed to the increase in density with additional amounts of thrombin, as denser clots were heavier and traveled with the greater percentage flowrate through the descending aorta. Because of the nature of fabricating the EAs, the volume was kept constant when calculating EA density; therefore, the increase in density among the EAs can be attributed to an increase in mass.

There was an increase in the number of trajectories through the CCAs with increasing thrombin concentration and AF flow conditions (Figure 4C). The percentage of EAs that traveled through the CCAs was lower than the percentage flowrate of 12% (9% under healthy flow conditions and 11% under AF flow conditions) at 5 NIHU but gradually increased with increasing thrombin concentration at 20 NIHU (13% under healthy flow conditions and 16% under AF flow conditions). The normal cardiac output was scaled down for the AF flow conditions with a corresponding reduction in pulse rate. This reduction in pulse rate may explain the increase in clots traveling towards the branching vessels as peak flow rates occurred more frequently than the normal flow rates, with 2 recurring peaks. This AF flow impacted the clots at an increased rate, as was observed by video evidence.

Although unusual, multiple emboli and associated cerebral infarcts have previously been recorded.[39,40] Multiple stroke occurrences can be attributed specifically to cardiogenic emboli.[41,42] Injecting more clots into the system increased the probability of at least 1 clot traveling along an aortic arch branching vessel. This probability was further increased under AF flow conditions. This is most evident when more clots were released into the system. Under healthy flow conditions, no more than 3 clots at a time traveled through the branching vessels. Under AF flow conditions, 4 and 5 clots traveled through the branching vessels 11% and 6% of the time, respectively. In 8% of tests, multiple clots traveled through the same branching vessel during a single test. Our observations show that multiple breakaway clots increase the chances of stroke-causing cardiogenic emboli. Menke et al,[6] reported cases of retrieved clots of up to 4 cm in length. These larger length clots are more likely to be caused by multiple clot formation rather than a large singular breakaway embolus of >30 mm in length.

One test or 1 iteration for each of the following scenarios was simulated; (1) position (left, right, anterior), (2) clot composition (0–20 NIHU), (3) 2 flowrate types (Healthy and AF), and (4) multiple released clots (from 1 to 5). In total, over 900 clots were released. Future tests should repeat some if not all of these scenarios at least 3×. Unfortunately, because of the time constraints, it took ≈5 minutes to release, record, remove, and prepare for the next test.

A limitation of this study was that the data used for AF flow conditions was scaled down from a healthy blood flowrate profile. A variation in AF flow profiles would allow for a much broader understanding of the irregular heartbeat and its effect on blood clot trajectory patterns. Outlet flowrate splits were also not given for this patient case. It is also noted that the composition of the clot for this patient case was unknown. Only one aortic arch configuration was analyzed. Further studies should include a range of patient-specific aortic arches to understand fully the geometric factors that influence clot trajectory paths.

Our study assumed cardiac source emboli. Aortic arch[43] and carotid artery[44] atherosclerosis are also likely sources of emboli. As the model is an exact cast of the arch and the branching vessels, no narrowing of the aortic arch or carotid arteries was visible in the computed tomography scan, so it can be assumed that cardiogenic embolism was the most likely source/cause. For the multiple breakaway emboli tests, a variation in clot type should be included to investigate the influence of clot size/density on clot trajectory paths.

The experimental system does not use bovine plasma but rather suspends the thrombi in a simple fluid without the normal circulating hemostatic and coagulation systems. Therefore, plasma coagulation factors, cofactors, and inhibitors do not participate in the fate of these thrombi, and there is no endothelium to interact with the thrombi. It should be noted that one might expect different outcomes should a biological fluid be used. Our test system requires 5 to 7 L of fluid. This amount of blood/plasma would be a biohazard because of an increased risk of infectious agents associated with this amount of flowing mammalian fluid and associated contamination risk within the rig. Because of this biohazard, a certified biological laboratory environment with a regulated sterile test system would be required. Also, blood is opaque, and this would prevent visualization of the clot trajectory paths. The viscosity of plasma is 3× to 4× lower than blood which would alter hemodynamic flow patterns, possibly altering the trajectory paths. The duration of the trajectory paths lasted only 2 to 3 s, which may not be of a sufficient time for a noticeable biological reaction.

Sources of Funding

This study was supported by Galway-Mayo Institute of Technology seed funding.

Disclosures

None.

References

1. Kelley RE, Minagar A. Cardioembolic stroke: an update. *South Med J*. 2003;96:343–349. doi: 10.1097/01.SMJ.0000063471.13035.85
2. Kannel WB, Benjamin EJ. Status of the epidemiology of atrial fibrillation. *Med Clin North Am*. 2008;92:17–40, ix. doi: 10.1016/j.mcna.2007.09.002
3. Beldi G, Beng L, Siegel G, Bisch-Knaden S, Candinas D. Prevention of perioperative thromboembolism in patients with atrial fibrillation. *Br J Surg*. 2007;94:1351–1355. doi: 10.1002/bjs.5835
4. Blackshear JL, Odell JA. Appendage obliteration to reduce stroke in cardiac surgical patients with atrial fibrillation. *Ann Thorac Surg*. 1996;61:755–759. doi: 10.1016/0003-4975(95)00887-X
5. Choi HW, Navia JA, Kassab GS. Stroke propensity is increased under atrial fibrillation hemodynamics: a simulation study. *PLoS One*. 2013;8:e73485. doi: 10.1371/journal.pone.0073485
6. Menke J, Lüthje L, Kastrup A, Larsen J. Thromboembolism in atrial fibrillation. *Am J Cardiol*. 2010;105:502–510. doi: 10.1016/j.amjcard.2009.10.018
7. Chung EM, Hague JP, Chanrion MA, Ramnarine KV, Katsogridakis E, Evans DH. Embolus trajectory through a physical replica of the major cerebral arteries. *Stroke*. 2010;41:647–652. doi: 10.1161/STROKEAHA.109.574400
8. Fahy P, Malone F, McCarthy E, McCarthy P, Thornton J, Brennan P, et al. An in vitro evaluation of emboli trajectories within a three-dimensional

physical model of the circle of willis under cerebral blood flow conditions. *Ann Biomed Eng*. 2015;43,2265–2278.
9. Wijman CA, Babikian VL, Winter MR, Pochay VE. Distribution of cerebral microembolism in the anterior and middle cerebral arteries. *Acta Neurol Scand*. 2000;101:122–127.
10. Gács G, Fox AJ, Barnett HJ, Vinuela F. CT visualization of intracranial arterial thromboembolism. *Stroke*. 1983;14:756–762.
11. Ou P, Celermajer DS, Mousseaux E, Giron A, Aggoun Y, Szezepanski I, et al. Vascular remodeling after "successful" repair of coarctation: impact of aortic arch geometry. *J Am Coll Cardiol*. 2007;49:883–890. doi: 10.1016/j.jacc.2006.10.057
12. Demertzis S, Hurni S, Stalder M, Gahl B, Herrmann G, Van den Berg J. Aortic arch morphometry in living humans. *J Anat*. 2010;217:588–596. doi: 10.1111/j.1469-7580.2010.01297.x
13. Di Martino ES, Bohra A, Vande Geest JP, Gupta N, Makaroun MS, Vorp DA. Biomechanical properties of ruptured versus electively repaired abdominal aortic aneurysm wall tissue. *Int Soc Cardiovas Surg*. 2006; 43:570–576.
14. Raghavan ML, Kratzberg J, Castro de Tolosa EM, Hanaoka MM, Walker P, da Silva ES. Regional distribution of wall thickness and failure properties of human abdominal aortic aneurysm. *J Biomech*. 2006;39:3010–3016. doi: 10.1016/j.jbiomech.2005.10.021
15. Thubrikar M, Labrosse MR, Robicsek F, Al-Soudi J, Fowler B. Mechanical properties of abdominal aortic aneurysm wall. *J Med Eng Technol*. 2000;25:133–142.
16. Bekham R, Roberts KE, Bierhals AJ, Jocaobs ME, Edgar JD, Paniello RC, et al. Aortic arch compliance and idiopathic unilateral vocal fold paralysis. *J Appl Physiol*. 2017;123:303–309.
17. Reymond P, Merenda F, Perren F, Ruefenacht D, Stergiopulos N. Validation of a one-dimensional model of the systemic arterial tree. *Am Physiol Soc*. 2009;297:208–222.
18. Clark DM, Plumb VJ, Epstein AE, Kay GN. Hemodynamic effects of an irregular sequence of ventricular cycle lengths during atrial fibrillation. *J Am Coll Cardiol*. 1997;30:1039–1045.
19. Hennen B, Markwirth T, Scheller B, Schäfers HJ, Wendler O. Do changes in blood flow in the subclavian artery affect flow volume in IMA grafts after complete arterial revascularization with the T-graft technique? *Thorac Cardiovasc Surg*. 2001;49:84–88. doi: 10.1055/s-2001-11701
20. Tokuda Y, Song MH, Ueda Y, Usui A, Akita T, Yoneyama S, et al. Three-dimensional numerical simulation of blood flow in the aortic arch during cardiopulmonary bypass. *Eur J Cardiothorac Surg*. 2008;33:164–167. doi: 10.1016/j.ejcts.2007.11.021
21. Sato K, Ogoh S, Hirasawa A, Oue A, Sadamoto T. The distribution of blood flow in the carotid and vertebral arteries during dynamic exercise in humans. *J Physiol*. 2010;589:2847–2856.
22. Benim AC, Nahavandi A, Assmann A, Schubert D, Feindt P, Suh SH. Simulation of blood flow in human aorta with emphasis on outlet boundary conditions. *Appl Math Model*. 2011;35:3175–3188.
23. Bürk J, Blanke P, Stankovic Z, Barker A, Russe M, Geiger J, et al. Evaluation of 3D blood flow patterns and wall shear stress in the normal and dilated thoracic aorta using flow-sensitive 4D CMR. *J Cardiovasc Magn Reson*. 2012;14:84. doi: 10.1186/1532-429X-14-84
24. Malone F, MacCarthy E, Delassus P, Fahy P, Kennedy J, Fagan AJ, et al. The mechanical characterisation of Bovine Embolus Analogues under various loading conditions [published online March 27, 2018]. *Cardiovasc Eng Technol*. doi: 10.1007/s13239-018-0352-3
25. Chueh JY, Wakhloo AK, Hendricks GH, Silva CF, Weaver JP, Gounis MJ. Mechanical characterization of thromboemboli in acute ischemic stroke and laboratory embolus analogs. *AJNR Am J Neuroradiol*. 2011;32:1237–1244. doi: 10.3174/ajnr.A2485
26. Uflacker, R. *Atlas of Vascular Anatomy: An Angiographic Approach*. 2nd Ed. South Carolina: Lippincott Williams & Wilkins; 2007.
27. Leary MC, Caplan LR. Carioembolic stroke: an update on etiology, diagnosis and management. *Anna Indian Acad Neurol*. 2008;11:52–63.
28. Bogousslavsky J, Van Melle G, Regli F, Kappenberger L. Pathogenesis of anterior circulation stroke in patients with nonvalvular atrial fibrillation: the Lausanne Stroke Registry. *Neurology*. 1990;40:1046–1050.
29. Davie EW, Fujikawa K. Basic mechanisms in blood coagulation. *Annu Rev Biochem*. 1975;44:799–829. doi: 10.1146/annurev.bi.44.070175.004055
30. Duffy S, Farrell M, McArdle K, Thornton J, Vale D, Rainsford E, et al. Novel methodology to replicate clot analogs with diverse composition in acute ischemic stroke. *J Neurointerv Surg*. 2017;9:486–491. doi: 10.1136/neurintsurg-2016-012308
31. Robinson RA, Herbertson LH, Sarkar Das S, Malinauskas RA, Pritchard WF, Grossman LW. Limitations of using synthetic blood clots for measuring *in vitro* clot capture efficiency of inferior vena cava filters. *Med Devices (Auckl)*. 2013;6:49–57. doi: 10.2147/MDER.S42555
32. Schmitt C, Hadj Henni A, Cloutier G. Characterization of blood clot viscoelasticity by dynamic ultrasound elastography and modeling of the rheological behavior. *J Biomech*. 2011;44:622–629. doi: 10.1016/j.jbiomech.2010.11.015
33. Krasokha, NW, Theisen S, Reese P, Mordasini C, Brekenfeld J, Gralla J, et al. Mechanical properties of blood clots—a new test method. *Mat wiss uWerkstofftech*. 2010; 41:1019–1024.
34. Stone WH. The relation of human and cattle blood groups. *Transfusion*. 1962;2:172–177.
35. Pichler L. Parameters of coagulation and fibrinolysis in different animal species-a literature based comparison. *Vet Med Austria*. 2008;95:282–295.
36. Liebeskind DS, Sanossian N, Yong WH, Starkman S, Tsang MP, Moya AL, et al. CT and MRI early vessel signs reflect clot composition in acute stroke. *Stroke*. 2011;42:1237–1243. doi: 10.1161/STROKEAHA.110.605576
37. Kan I, Yuki I, Murayama Y, Vinuela FA, Kim RH, Vinters HV, et al. A novel method of thrombus preparation for use in a swine model for evaluation of thrombectomy devices. *AJNR Am J Neuroradiol*. 2010;31:1741–1743. doi: 10.3174/ajnr.A1991
38. Thambidorai SK, Murray RD, Parakh K, Shah TK, Black IW, Jasper SE, et al; ACUTE investigators. Utility of transesophageal echocardiography in identification of thrombogenic milieu in patients with atrial fibrillation (an ACUTE ancillary study). *Am J Cardiol*. 2005;96:935–941. doi: 10.1016/j.amjcard.2005.05.051
39. Chetwood A, Sanders A, Saweirs M, Thapar A, Davies AH. Multiple arterial emboli secondary to left ventricular thrombus in a 35-year-old obese male. *J Cardiovasc Dis Res*. 2010;1:203–205. doi: 10.4103/0975-3583.74264
40. Baird AE, Lövblad KO, Schlaug G, Edelman RR, Warach S. Multiple acute stroke syndrome: marker of embolic disease? *Neurology*. 2000;54:674–678.
41. Bogousslavsky J. Double infarction in one cerebral hemisphere. *Ann Neurol*. 1991;30:12–18. doi: 10.1002/ana.410300104
42. Geffroy M, Belden JR, Pessin MS, Caplan LR. Recurrent infarcts in different vascular territories in a brief period: a hypercoaguable state? *Neurology*. 1996;46(suppl):A141.
43. Kessler C, Mitusch R, Guo Y, Rosengart A, Sheikhzadeh A. Embolism from the aortic arch in patients with cerebral ischemia. *Thromb Res*. 1996;84:145–155.
44. Surov A, Behrmann C, Kornhuber M. Neurological picture. Carotid embolism. *J Neurol Neurosurg Psychiatry*. 2007;78:564. doi: 10.1136/jnnp.2006.105593